Conference paper

Susanne Bähr and Martin Oestreich*

The electrophilic aromatic substitution approach to C–H silylation and C–H borylation

https://doi.org/10.1515/pac-2017-0902

Abstract: Several approaches toward electrophilic C–H silylation of electron-rich arenes are discussed, comprising transition-metal-catalyzed processes as well as Lewis-acid- and Brønsted-acid-induced protocols. These methods differ in the catalytic generation of the silicon electrophile but share proton removal in form of dihydrogen. With slight modifications, these methods are often also applicable to the related electrophilic C–H borylation.

Keywords: boron electrophiles; C–H functionalization; cooperative catalysis; electrophilic aromatic substitution; IMEBORON-16; silicon electrophiles.

Introduction

Electrophilic aromatic substitution (S_EAr) is established synthetic methodology for the construction of C–C (and C–Het) bonds at sufficiently nucleophilic arenes **I** (Scheme 1, left). Friedel–Crafts alkylations proceed through Wheland intermediates **II** (**I**→**II**), and these convert into **III** by proton release (**II**→**III**). This can become an issue when the overall process is reversible, as it is the case for Friedel–Crafts alkylations and also for electrophilic C–H silylations (Scheme 1, right) [1]. In fact, the formation of Wheland intermediate **IV** by protonation of **V** is facile because **IV** is stabilized by the β-silicon effect. Hence, the backward reaction **V** to **IV** is favored over **II** from **III**. To avoid that protodesilylation (**V**→**IV**→**I**), irreversible proton removal would be the ideal solution. That means, put another way, the deliberate addition of base cannot be the solution to the problem as the resulting conjugate acid would likely be too acidic. The newly developed approaches achieve this proton removal by the generation and liberation of dihydrogen gas. With little modification, these methods are also applicable to the corresponding borylation reactions. We herein summarize our recent work on both the C–H silylation and C–H borylation by catalytic electrophilic aromatic substitution.

Ruthenium–sulfur complexes as catalysts

Dihydrogen activation at the metal–sulfur bond of the active site **1** in [NiFe] hydrogenases is likely to result in the formation of a metal hydride together with a protonated thiol ligand (Scheme 2, top) [2, 3]. Inspired by this naturally occuring example of metal–ligand cooperativity, Ohki and Tatsumi introduced rhodium(III) and iridium(III) complexes **2** and **3** (Scheme 2, bottom) [4]. The expected reactivity was indeed observed, and a

Article note: A collection of invited papers based on presentations at the 16th International Meeting on Boron Chemistry (IMEBORON-16), Hong Kong, 9–13 July 2017.

***Corresponding author: Martin Oestreich,** Institut für Chemie, Technische Universität Berlin, Strasse des 17. Juni 115, 10623 Berlin, Germany, e-mail: martin.oestreich@tu-berlin.de. http://orcid.org/0000-0002-1487-9218
Susanne Bähr: Institut für Chemie, Technische Universität Berlin, Strasse des 17. Juni 115, 10623 Berlin, Germany. http://orcid.org/0000-0001-5113-7646

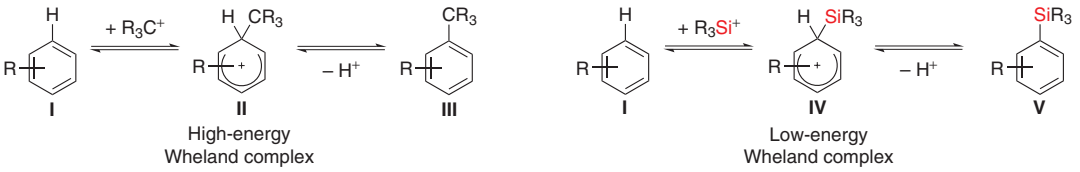

Scheme 1: Reversibility of electrophilic aromatic substitutions with carbon and silicon electrophiles.

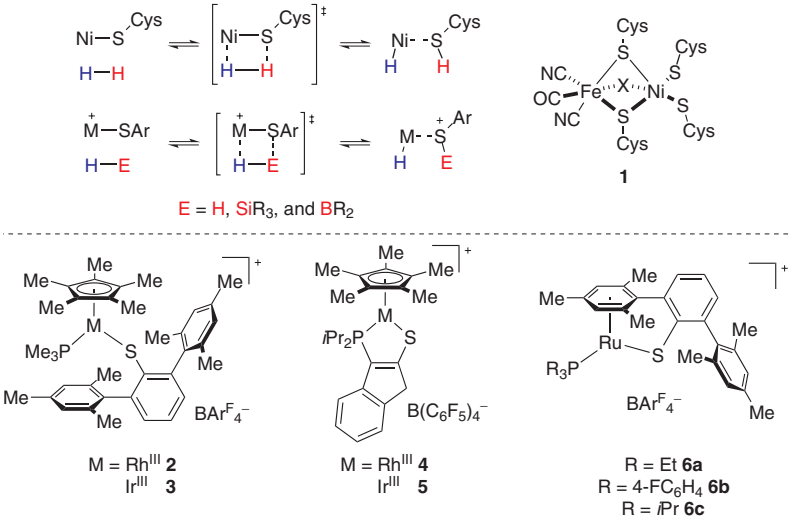

Scheme 2: Bioinspired concept (top) and transition-metal complexes (bottom) for the cooperative activation at metal–sulfur bonds (X = O or OH, Cys = cysteine, Ar^F = 3,5-bis(trifluoromethyl)phenyl).

complex resulting from H–H splitting was formed at low temperature by treatment of **3** with dihydrogen (not shown). In collaboration with Ohki and Tatsumi, our group anticipated that an analogous heterolytic activation of Si–H or B–H bonds would also result in a metal hydride together with a sulfur-stabilized silylium ion and borenium ion, respectively (Scheme 2, top). This assumption was supported by a report from Stradiotto

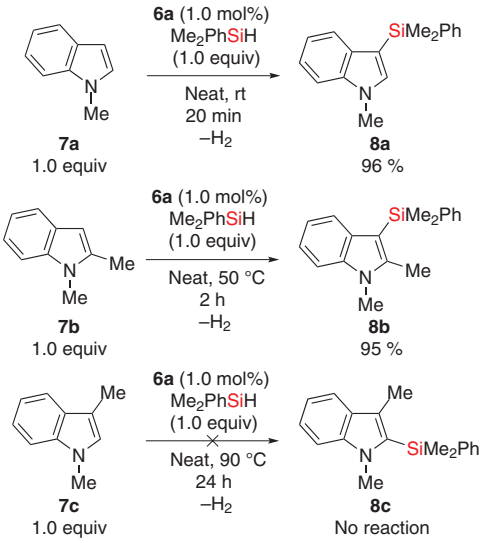

Scheme 3: Dehydrogenative silylation of indoles **7** catalyzed by **6a**.

and co-workers on rhodium(III) and iridium(III) complexes **4** and **5** with a bidentate P,S-ligand [5]. These compounds activate hydrosilanes in a cooperative fashion, and complex **4** showed also catalytic activity in the hydrosilylation of ketones (not shown). However, we observed decomplexation of the monodentate thiolate ligand upon treatment of complexes **2** or **3** with hydrosilanes [6]. This decomposition could be avoided by using ruthenium(II) complexes **6** with a bidentate thiolate ligand. This coordinatively unsaturated, cationic complex had previously been applied to dihydrogen activation by Ohki and Tatsumi with moderate efficacy [7] but emerged as a superb choice for the heterolytic splitting of the weaker Si–H bond [6, 8].

We envisioned that the sulfur-stabilized silylium ion obtained by hydrosilane activation with catalyst **6a** could be sufficiently electrophilic to engage in aromatic substitution reactions with electron-rich arenes such as indoles **7** (Scheme 3). The silylated indole **8a** was indeed formed when **7a** was treated with 1.0 mol% of **6a** in the presence of Me_2PhSiH (**7a**→**8a**) [6]. In accordance with an electrophilic aromatic substitution mechanism, exclusive C3 selectivity was observed. Also, C2-substituted **7b** was successfully applied (**7b**→**8b**) whereas substitution at C3 as in **7c** prevented the reaction, and **8c** was not formed, corroborating electronic control as the regiocontrolling factor.

The catalytic cycle of this transformation commences with cooperative Si–H bond activation across the polar metal–sulfur bond of cationic complex **6** (Scheme 4, left) [9]. Depending on the steric demand of the hydrosilane, η^1 or η^2 coordination of the hydrosilane to the ruthenium center in **9** precedes the heterolysis of the Si–H bond (**6** + *Si*–H→**9**→**10**). As supported by DFT calculations, the activation results in the formation of a metal hydride and a sulfur-stabilized silylium ion in **10** by way of **TS1** (Scheme 4, top right). This metathesis step is significantly lower in energy compared to the alternative transition state **TS2** (13.4 kJ/mol vs. 48.5 kJ/mol) that would result in the corresponding regioisomeric complex. From **10**, silyl transfer onto indole **7** results in the formation of the neutral hydride **11** (**10**→**11**). Subsequent deprotonation leads to C3-silylated **8** and dihydrogen adduct **12** (**11**→**12**). Release of dihydrogen closes the catalytic cycle concomitant with the regeneration of **6** (**12**→**6** + H_2). It must be noted that all steps are reversible, and hydrogen evolution shifts the equilibrium to the side of the dehydrogenative coupling.

We were later able to adapt this dehydrogenative C–H silylation method to intramolecular reactions. It had been shown that dibenzosiloles **14** can be synthesized involving intermediate silicon electrophiles

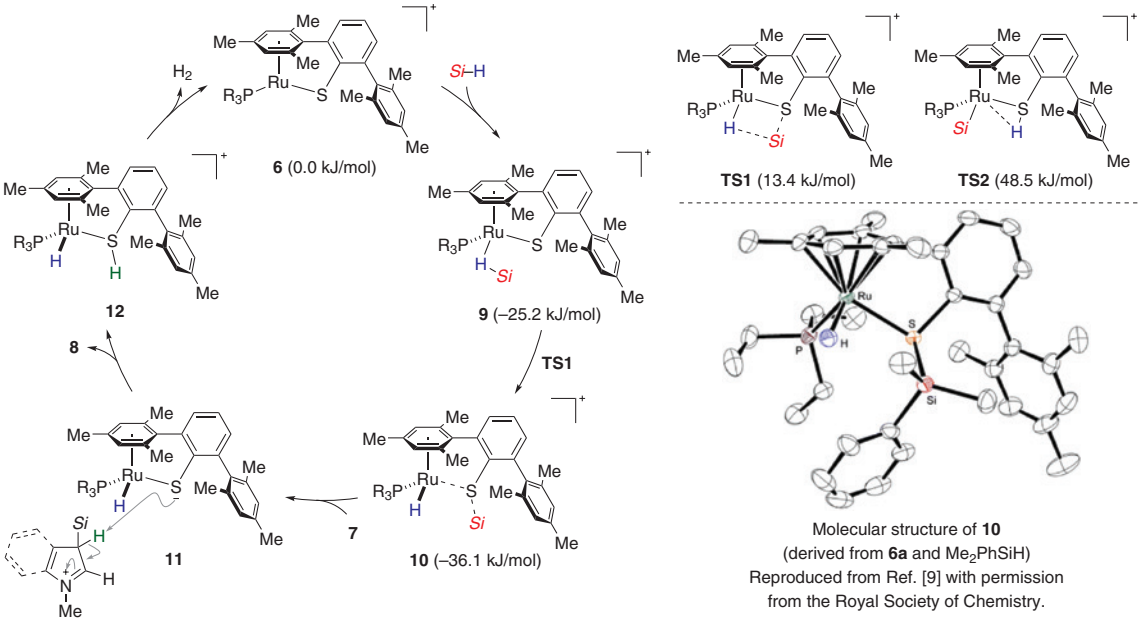

Scheme 4: Mechanism of the Si–H bond activation and S_EAr (left), competing transition states **TS1** and **TS2** of the Si–H bond activation (top right), and molecular structure of adduct **10** (bottom right). Energy values and molecular structure are shown for *Si* = $SiMe_2Ph$ and R = Et. H atoms except for Ru–H and the counteranion have been omitted for clarity.

that are accessed either stoichiometrically [10, 11] or – with limited scope though – catalytically [12]. We envisioned that **6** could also serve as suitable catalyst for the formation of dibenzosiloles **14**. Ruthenium(II) complex **6b** with an electron-deficient phosphine ligand turned out to be the best choice for this ring closure (Scheme 5) [13]. However, significantly higher temperatures were needed due to the lower nucleophilicity of the arenes, and the reversibility was now a serious challenge: dihydrogen activation with **6** led to incomplete conversions of the hydrosilanes **13**. Key to success was microwave heating together with perforated caps to ensure the release of dihydrogen gas. Substituents such as alkyl or aryl groups as well as halogen atoms were tolerated (not shown) but the particular value of this method lies in the possibility to access dibenzosiloles **14a–c** that are functionalized at both phenylene groups. Silole **15**, obtained in three steps from the corresponding *tert*-butyldimethylsilyl-protected hydrosilane by cyclization, deprotection, and triflation, would even allow for site-selective cross-coupling. A combination of both aforementioned approaches, that is intermolecular indole C3 silylation and intramolecular benzosilole formation, enabled a facile synthesis of indole-fused benzosiloles from readily available precursors, not requiring any prefunctionalization (not shown) [14].

In analogy to the Si–H bond activation, we later showed that using a hydroborane together with catalyst **6** allows for the formation of stabilized borenium ions in **16** (**6** + *B*–H→**16**, Scheme 6, left) [15]. The corresponding B–H adduct **16** was crystallographically characterized, and we succeeded in the borylation of **7** with pinBH (**7**→**17**), leading for example to C3-borylated indole **17a** and pyrrole **17d** (Scheme 6, right). Again, the reaction of **7** proceeded with high regioselectivity and in good to excellent yields, and Lewis-basic

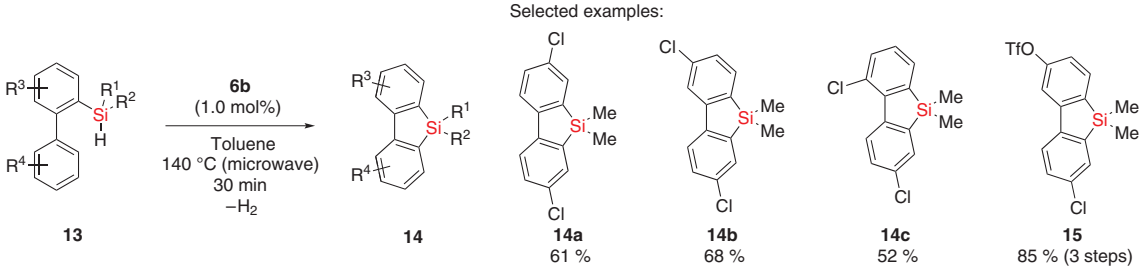

Scheme 5: Catalytic S_EAr approach toward dibenzosiloles with **6b** as catalyst (Tf = trifluoromethanesulfonyl).

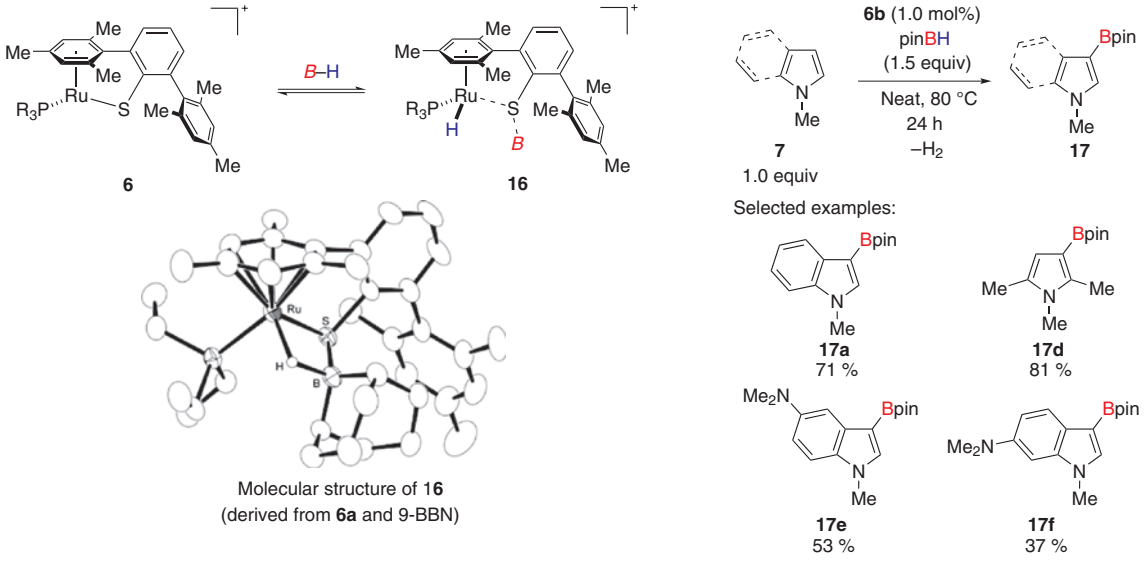

Scheme 6: Access to borane adduct **16** and molecular structure thereof (left) as well as selected examples for the catalytic borylation of **7** (right). H atoms except for Ru–H and counteranion have been omitted for clarity.

functionalities such as amino groups in **17e** and **17f** were tolerated. It is a rare example of an S_EAr with pinBH; usually catBH is used in electrophilic C–H borylation followed by transesterification with pinacol.

When we applied imines **18** [16, 17] as substrates for catalysts **6** together with hydrosilanes, we expected two major reaction pathways (Scheme 7, left): ruthenium hydride **11** either serves as a reductant for the iminium-ion intermediates **19** (**18**→**19**) to yield the corresponding *N*-silylated amines **20** (**19** + **11**→**20** + **6**, left pathway). Alternatively, the basic sulfur atom in **11** could deprotonate at the acidified α position in **19**, leading to *N*-silylated enamines **21** (**19** + **11**→**21** + **6**·H_2, right pathway). The formation of **20** was largely suppressed by performing the reaction in open vessels to ensure removal of the dihydrogen gas [16]. Hence, **21a** (**18a**→**21a**, Scheme 7, right) was obtained as major product when imine **18a** was treated with Me_2PhSiH (1 equiv) in the presence of catalyst **6c** along with disilylated **22a** in trace amounts. The latter results from electrophilic silylation of **21** at its nucleophilic β carbon atom and subsequent deprotonation at the same position, a reaction similar to the silylation of indoles **7** (cf. Scheme 3). Changing to the bulkier substrate **18b** and applying 2 equivalents of hydrosilane resulted in the almost exclusive formation of disilylated enamine **22b** (**18b**→**22b**).

We also accomplished the 1,4-hydrosilylation of pyridines **23** to dihydropyridines **24** (**23**→**24**, Scheme 8) with catalysts **6** [18]. The proposed mechanism starts again with hydrosilane activation (**6** + *Si*–H→**10**, Scheme 8, left). Silyl transfer from **10** onto the Lewis-basic pyridine **23a** results in the formation of a pyridinium ion and ruthenium hydride **11**. Regioselective hydride transfer affords the 1,4-dihydropyridine **24a** exclusively, and **24a** was isolated in high yield (Scheme 8, right); no 1,2-isomer or overreduced products were observed. Mono- and disubstituted dihydropyridines **24b** or **24c** were successfully synthesized as well. Remarkably, and in contrast to a related work from Nikonov and co-workers [19], substituents in the C4 position of the pyridine did not thwart the reaction, and **24d** was isolated in good yield.

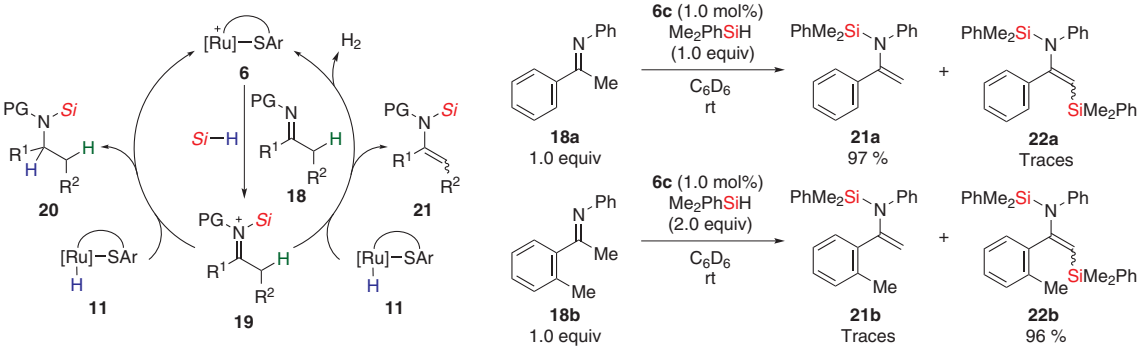

Scheme 7: Hydrosilylation vs. dehydrogenative coupling of imines **18** (PG = protective group). The counteranion has been omitted for clarity.

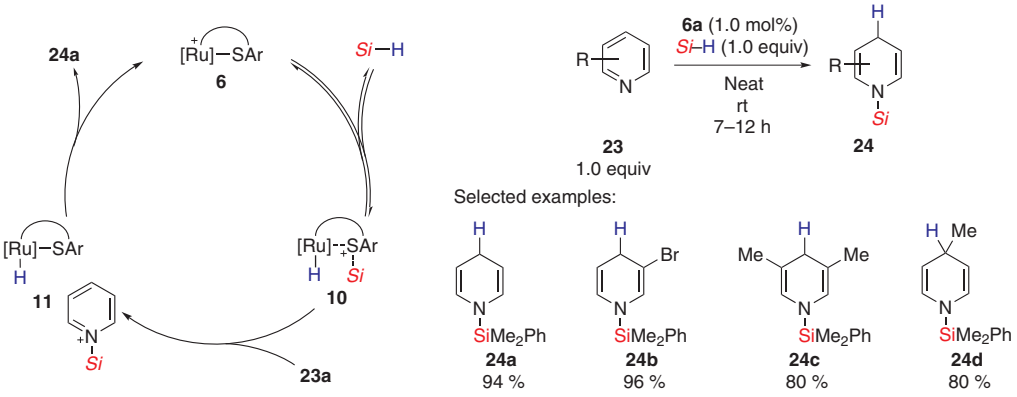

Scheme 8: Simplified mechanism (left) and selected examples (right) for the 1,4-hydrosilylation of pyridines **23**.

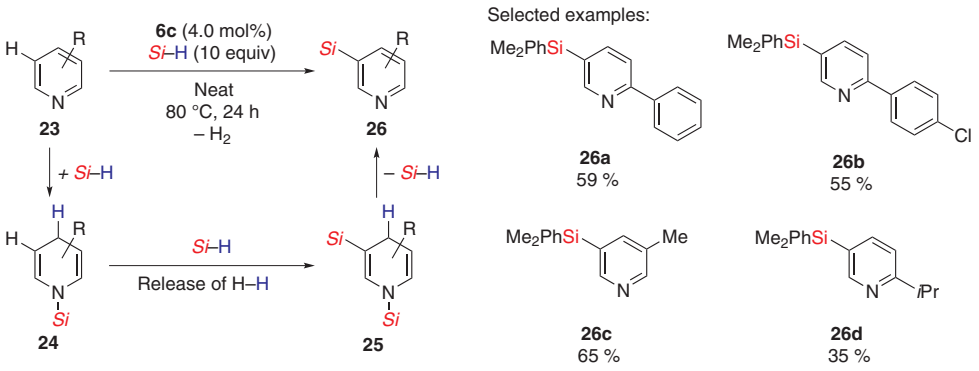

Scheme 9: C–H silylation of pyridines **23** by temporary dearomatization (left) and selected examples (right).

The dihydropyridine core in **24** resembles the structural element of two *N*-silylated enamines. We reasoned that electrophilic silylation in the β position of **24** (as in the disilylation of imines **18**, cf. Scheme 7, right) and subsequent 1,4-dehydrosilylation of **25** would result in the formation of pyridines **26** silylated in the *meta* position (Scheme 9, left). As a consequence of the temporary dearomatization, the overall process can be viewed as a formal electrophilic aromatic substitution of pyridines **23**. With **6c** as catalyst, several silylated pyridines **26** (**23**→**26**), usually substituted with an aryl group in the *ortho* position as in **26a** and **26b**, were successfully synthesized (Scheme 9, right) [20]. Also, alkyl substituents as in **26c** and **26d** were tolerated, even though the products were obtained in lower yields. Deuterium-labeling as well as NMR measurements proved the stepwise sequence of 1,4-hydrosilylation, dehydrogenative silylation, and rearomatization (not shown).

Base-metal salts and boron Lewis acids for electrophilic C–H functionalization

Inspired by established catalysts for Friedel–Crafts chemistry, we focused on metal salts such as iron chlorides for the silylation by way of electrophilic aromatic substitution. We found that aniline derivatives **27** as electron-rich arenes are suitable for the conversion to **28** with hydrosilanes applying $FeCl_2$ together with $NaBAr^F_4$ as initiator (**27**→**28**, Scheme 10) [21]; **28a–c** were isolated in moderate to high yields. Substitution in the *para* position as in **27d** prevented the reaction, and **28d** did not form. Other metal salts, including Fe(III), Sc(III), Co(II), Cu(II), Zn(II), Al(III), Y(III), Ce(III), Sm(III), and In(III) triflates and chlorides, were equally effective.

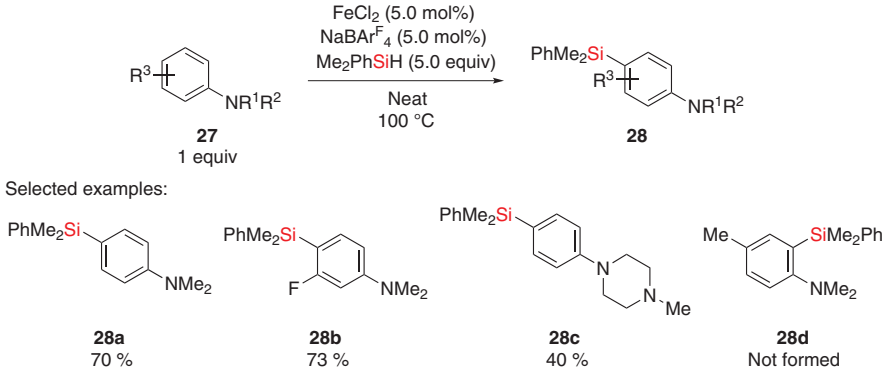

Scheme 10: Selected examples for base-metal-salt-initiated silylation of anilines **27**.

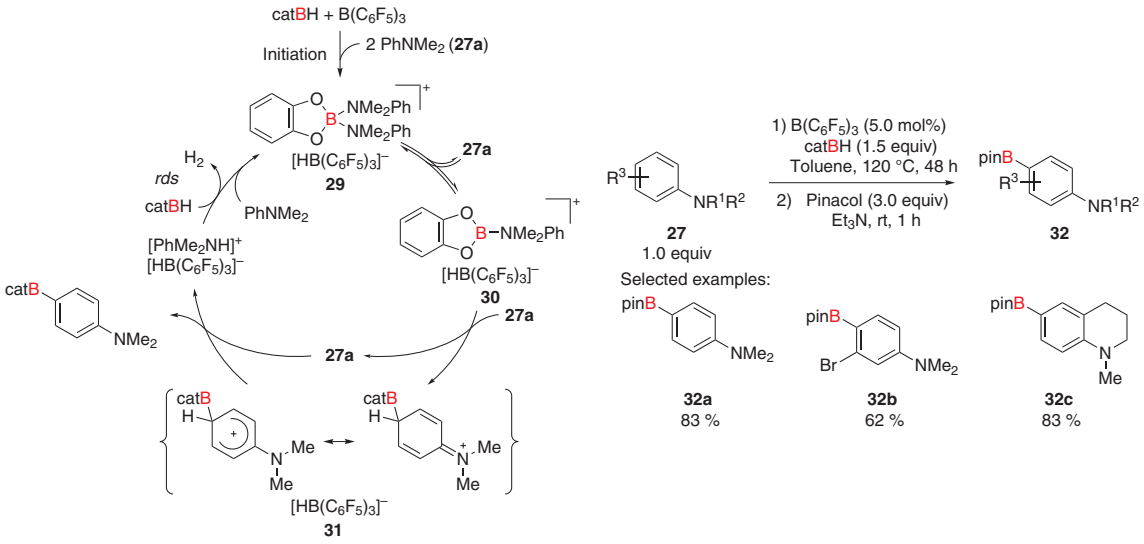

Scheme 11: Catalytic cycle for the borane-initiated borylation of anilines **27** (left) and selected examples (right).

Even though the nature of the catalyst is unclear, we reasoned that initial borane formation from the borate counteranion caused by the metal salt could be operative; such reaction was reported with noble metal complexes of platinum(II) [22], rhodium(III) [23], and gold(I) [24]. Electron-deficient boranes are suitable catalysts for such a transformation, as independently shown by Hou and co-workers [25] who disclosed the dehydrogenative C–H silylation of anilines **27** with $B(C_6F_5)_3$ as catalyst. Based on that publication, also the related borylation using $B(C_6F_5)_3$ in catalytic amounts was recently achieved by our laboratory (Scheme 11) [26]. The mechanism involves boronium ion **29** that is formed by hydride abstraction with $B(C_6F_5)_3$ from catecholborane and coordination of two substrate molecules (Scheme 11, left). Decoordination leads to borenium ion **30** (**29**→**30**) that reacts with aniline **27a** to arrive at Wheland intermediate **31** (**30**→**31**). Deprotonation by the substrate forms the borylated arene together with an ammonium salt. The subsequent release of dihydrogen to regenerate **29** is likely to be the rate-determining step. Dramatic rate acceleration by added alkenes is observed (not shown), even though the effect of that additive is not understood. Anilines **27** reacted in moderate to good yields to borylated **32** after transesterification with pinacol (**27**→**32**, Scheme 11, right). Indoles **7** participated as well (not shown) [27].

Brønsted-acid-promoted dehydrogenative C–H silylation

A fundamentally different approach to access (stabilized) silylium ions is based on inital work by Corey and co-workers [28], in which the formation of a trialkylsilyl triflate by treatment of the corresponding hydrosilane with triflic acid was reported (Scheme 12, top left). The transfer of this procedure to aryl-substituted hydrosilanes failed due to protodesilylation; the silyltriflate was obtained together with benzene in this case (not shown) [29]. Our group succeeded in the formation of ether-stabilized, aryl-substituted silylium ions by changing to Brookhart's acid [30] as the proton source (Scheme 12, bottom left) [31].

We were also able to catalytically access the stabilized silylium ion and apply it to the conversion of indoles **7** to silylated **33** (**7**→**33**). Ph_2SiH_2 was chosen in order to have a handle for further functionalization at the silicon atom, and norbornene was found to be essential to secure consistently high yields. Its fate is most likely proton-induced oligomerization. Complete C3 selectivity in **33a** was observed, and the C2-substituted indole **33b** was also converted in high yield although indole-to-indoline reduction by dihydrogen remains a limitation for both. Again, a substituent in C3 thwarted the reaction, and **33c** did not form.

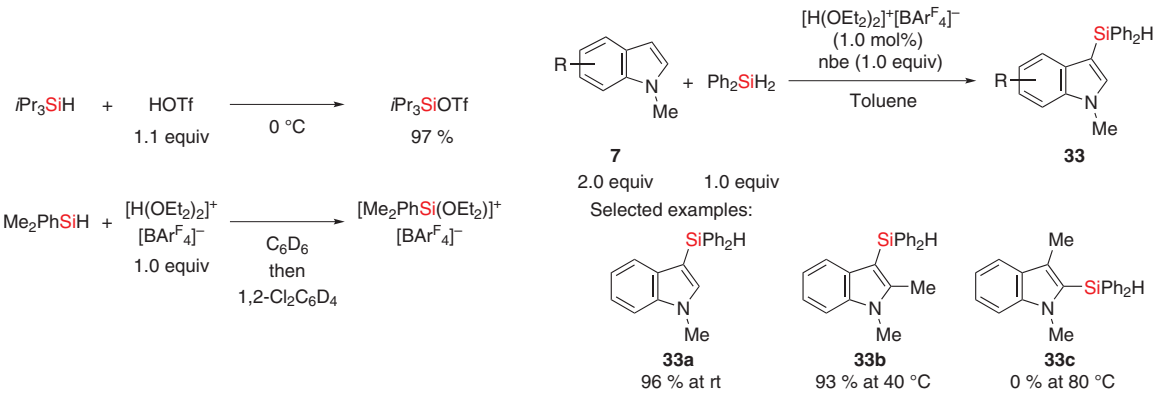

Scheme 12: Brønsted acids for the formation of stabilized silylium ions (left) and application to the electrophilic C–H silylation of indoles (right, nbe = norbornene).

Conclusion

Owing to the advances made in recent years, S_EAr with silicon and boron electrophiles changed from a basic concept to a useful methodology. The advantage lies in easily available starting materials, and the formation of dihydrogen as the sole byproduct. However, limitations remain with regard to narrow functional-group tolerance, especially in case of highly electrophilic and oxophilic silicon intermediates. Furthermore, usually only electron-rich and, hence, nucleophilic arenes engage in these substitution reactions. These drawbacks, however, are the basis for further developments in this promising area.

Acknowledgement: S.B. thanks the Studienstiftung des deutschen Volkes for a predoctoral fellowship (2015–2018), and M.O. is indebted to the Einstein Foundation (Berlin) for an endowed professorship. We particularly thank Dr. Qing-An Chen, Dr. Julia Hermeke, Dr. Hendrik F. T. Klare, Dr. C. David F. Königs, Dr. Kristine Müther, Lukas Omann, Dr. Timo Stahl, Simon Wübbolt, and Dr. Qin Yin for their enthusiasm and commitment. We are also grateful to Professors Ohki and Tatsumi for the fruitful collaboration and hosting stays of H.F.T.K., C.D.F.K., and K.M. within the framework of the International Research Training Group Münster–Nagoya (GRK 1143 of the Deutsche Forschungsgemeinschaft).

References

[1] S. Bähr, M. Oestreich. *Angew. Chem. Int. Ed.* **56**, 52 (2017).
[2] P. M. Vignais, B. Billoud. *Chem. Rev.* **107**, 4206 (2007).
[3] J. C. Fontecilla-Camps, A. Volbeda, C. Cavazza, Y. Nicolet. *Chem. Rev.* **107**, 4273 (2007).
[4] Y. Ohki, M. Sakamoto, K. Tatsumi. *J. Am. Chem. Soc.* **130**, 11610 (2008).
[5] A. K. D. Hesp, R. McDonald, M. J. Ferguson, M. Stradiotto. *J. Am. Chem. Soc.* **130**, 16394 (2008).
[6] H. F. T. Klare, M. Oestreich, J.-i. Ito, H. Nishiyama, Y. Ohki, K. Tatsumi. *J. Am. Chem. Soc.* **133**, 3312 (2011).
[7] Y. Ohki, Y. Takikawa, H. Sadohara, C. Kesenheimer, B. Engendahl, E. Kapatina, K. Tatsumi. *Chem. Asian J.* **3**, 1625 (2008).
[8] For an account on cooperative activation of E–H bonds (with E = H, B, and Si) with catalysts **6**, see: L. Omann, C. D. F. Königs, H. F. T. Klare, M. Oestreich. *Acc. Chem. Res.* **50**, 1258 (2017).
[9] T. Stahl, P. Hrobárik, C. D. F. Königs, Y. Ohki, K. Tatsumi, S. Kemper, M. Kaupp, H. F. T. Klare, M. Oestreich. *Chem. Sci.* **6**, 4324 (2015).
[10] S. Furukawa, J. Kobayashi, T. Kawashima. *J. Am. Chem. Soc.* **131**, 14192 (2009).
[11] S. Furukawa, J. Kobayashi, T. Kawashima. *Dalton Trans.* **39**, 9329 (2010).
[12] L. D. Curless, M. J. Ingleson. *Organometallics* **33**, 7241 (2014).
[13] L. Omann, M. Oestreich. *Angew. Chem. Int. Ed.* **54**, 10276 (2015).
[14] L. Omann, M. Oestreich. *Organometallics* **36**, 767 (2017).
[15] T. Stahl, K. Müther, Y. Ohki, K. Tatsumi, M. Oestreich. *J. Am. Chem. Soc.* **135**, 10978 (2013).

[16] J. Hermeke, H. F. T. Klare, M. Oestreich. *Chem. Eur. J.* **20**, 9250 (2014).
[17] The dehydrogenative coupling of ketones with **6a** was also accomplished in our group: C. D. F. Königs, H. F. T. Klare, Y. Ohki, K. Tatsumi, M. Oestreich. *Org. Lett.* **14**, 2842 (2012).
[18] C. D. F. Königs, H. F. T. Klare, M. Oestreich. *Angew. Chem. Int. Ed.* **52**, 10076 (2013).
[19] D. V. Gutsulyak, A. van der Est, G. I. Nikonov. *Angew. Chem. Int. Ed.* **50**, 1384 (2011).
[20] S. Wübbolt, M. Oestreich. *Angew. Chem. Int. Ed.* **54**, 15876 (2015).
[21] Q. Yin, H. F. T. Klare, M. Oestreich. *Angew. Chem. Int. Ed.* **55**, 3204 (2016).
[22] W. V. Konze, B. L. Scott, G. J. Kubas. *Chem. Commun.* 1807 (1999).
[23] H. Salem, L. J. W. Shimon, G. Leitus, L. Weiner, D. Milstein. *Organometallics* **27**, 2293 (2008).
[24] S. G. Weber, D. Zahner, F. Rominger, B. F. Straub. *Chem. Commun.* **48**, 11325 (2012).
[25] Y. Ma, B. Wang, L. Zhang, Z. Hou. *J. Am. Chem. Soc.* **138**, 3663 (2016).
[26] Q. Yin, H. F. T. Klare, M. Oestreich. *Angew. Chem. Int. Ed.* ***56***, 3712 (2017).
[27] For a related work, see: F. Kitani, R. Takita, T. Imahori, M. Uchiyama. *Heterocycles* **95**, 158 (2017).
[28] E. J. Corey, H. Cho, C. Rücker, D. H. Hua. *Tetrahedron* **22**, 3455 (1981).
[29] A. R. Bassindale, T. Stout. *J. Organomet. Chem.* **271**, C1 (1984).
[30] M. Brookhart, B. Grant, A. F. Volpe, Jr. *Organometallics* **11**, 3920 (1992).
[31] Q.-A. Chen, H. F. T. Klare, M. Oestreich. *J. Am. Chem. Soc.* **138**, 7868 (2016).